Sensors and Actuators B 186 (2013) 278–285

Contents lists available at SciVerse ScienceDirect

Sensors and Actuators B: Chemical

journal homepage: www.elsevier.com/locate/snb

A novel fluorescent probe based on rhodamine B derivative for highly selective and sensitive detection of mercury(II) ion in aqueous solution

Jingkai Ni[a,b], Qiuyan Li[c], Bin Li[a,*], Liming Zhang[a]

[a] State Key Laboratory of Luminescence and Applications, Changchun Institute of Optics Fine Mechanics and Physics, Chinese Academy of Sciences, Changchun 130033, PR China
[b] University of Chinese Academy of Sciences, Beijing 100039, PR China
[c] Changchun Institute of Engineering Technology, Changchun 130017, PR China

ARTICLE INFO

Article history:
Received 29 January 2013
Received in revised form 13 May 2013
Accepted 3 June 2013
Available online 14 June 2013

Keywords:
Rhodamine B
Hg^{2+} sensing
Fluorescent
Colorimetric

ABSTRACT

In the present work, a new rhodamine B Schiff base 3′,6′-bis(diethylamino)-2-(2-oxoethylideneamino)-spiro[isoindoline-1,9′-xanthen]-3-one (RHO) was designed and easily prepared as a Hg^{2+} fluorescent and colorimetric probe, which could selectively and sensitively detect Hg^{2+} in 7:3 (v/v) ethanol–water solution by showing enhanced fluorescence emission. Meanwhile distinct color change from colorless to pink also provided "naked eye" detection of Hg^{2+} owing to the ring opening of spirolactam of the rhodamine derivative. Other ions including alkali and alkaline earth metal ions (K^+, Mg^{2+}, and Ca^{2+}), and some transition metal ions (Ni^{2+}, Co^{2+}, Fe^{2+}, Cu^{2+}, Zn^{2+}, Cd^{2+}, Ag^+, Pb^{2+}, Cr^{3+}, and Fe^{3+}) could hardly induce any interference. For further use in practical applications in optical ion sensing devices, we immobilized the probe onto silica spheres to explore its functionality in inorganic and organic hybrid materials. As a result, excellent discrimination of Hg^{2+} from other cations could also be obtained.

1. Introduction

Mercury is known as a highly toxic element and spreads widely in the environment. Mercury contamination occurs through a diverse range of natural and anthropogenic sources, including ocean and volcanic eruption [1,2], gold mining, waste incineration, and combustion of fossil fuels. Under the action of bacteria, both elemental and ionic mercury in the environment can bioaccumulate through the food chain [3]. What's worse, due to mercury's high affinity for thiol group in proteins and enzymes, even low dose exposure can lead to the dysfunction of cells and consequently cause many health problems in brain, kidney, central nervous, mitosis and endocrine system [4,5]. Hence, there is a high demand for selective and sensitive detecting method for tracking hazard mercury.

Although traditional analytical techniques such as atomic absorption spectrometry (AAS), atomic fluorescence spectrometry (AFS) and inductively coupled plasma-mass spectrometry (ICP-MS) have been applied to detect the concentration of mercury, the wide utilization of these methods is largely limited due to the expensive equipment and time consuming sample preparation procedures. In view of these sophisticated experimental methods, many efforts have been devoted to pursue an innovative and convenient sensor material for detection of mercury(II) which can offer high sensitivity and selectivity.

Owing to the rapid detection, easy handling and simple equipment, much effort has been paid to the development of fluorogenic and chromogenic chemosensors that can selectively respond to mercury(II) ion [6–11]. Among these sensors, rhodamine derivatives have been widely employed due to their long absorption and emission wavelengths, high extinction coefficient and high fluorescence quantum yield [12–14]. Rhodamine based chemosensors can display not only obvious absorbance and fluorescence intensity changes toward some specific metal ions, but also induce a strong color change during the sensing event, facilitating "naked eye" detection. The sensing mechanism is based on the transformation.

of non-fluorescent spirocyclic form to the ring-opened amide form which is pink and highly fluorescent. The cost-effective fluorescent probes based on rhodamine derivatives for mercury(II) ion have been reported by some research groups [15–17]. Unfortunately, most of the reported chemosensors have some disadvantages, such as strict reaction condition, complicated synthetic route or cross-sensitivities toward other metal ions, or in order to take advantage of the thiophilicity of Hg^{2+}, sulfur was often introduced into the responding unit ignoring its negative

* Corresponding author. Tel.: +86 431 86176935; fax: +86 431 86176935.
E-mail address: libinteacher@163.com (B. Li).

0925-4005/$ – see front matter © 2013 Elsevier B.V. All rights reserved.
http://dx.doi.org/10.1016/j.snb.2013.06.011

Fig. 1. Visual color changes of RHO (10 μM) with addition of 5 equiv. of different metal ions in ethanol/water (7:3, v/v), from left to right, the sequence of ions added were Hg^{2+}, K^{+}, Mg^{2+}, Fe^{3+}, Cd^{2+}, Co^{2+}, Ca^{2+}, Zn^{2+}, Ni^{2+}, Fe^{2+}, Pb^{2+}, Cr^{3+}, Cu^{2+} and Ag^{+}.

influence toward natural systems. Here, our study is to utilize simple molecules as platform to facilitate the reaction, the obtained nontoxic fluorescent probe possess highly selective and rapid spectroscopic response to Hg^{2+} in aqueous media.

In this context, we report a novel but simple fluorescent probe based on rhodamine B derivative, it can discriminate Hg^{2+} from the other common cations by fluorescent and chromogenic analyses in aqueous solutions with high selectivity and sensitivity, obvious color change from colorless to pink also provided "naked eye" detection. For practical applications in optical ion sensing devices, it is necessary to incorporate the probe molecule into a solid matrix. When grafted onto inorganic matrix of silica spheres, though the terminal O was replaced by imine N, it also acted as an excellent Hg^{2+} fluorescent probe and maintain the high selectivity.

2. Experimental

2.1. Materials and equipments

All analytical grade chemicals were used as received without further purification. Deionized water was used in this work. The solutions of metal ions were prepared from their corresponding nitrate salts. And all the fluorescent and UV–vis analyses were conducted 25 min later when Hg^{2+} was added into the solution. We chose ethanol–water 7:3 (v/v) as the test solution in order to improve the solubility and sensitivity of the probe.

The UV–vis absorption spectra were obtained on a Shi-madzu-UV-3101 scanning spectrophotometer. Fluorescence spectra were measured with a Hitachi F-4500 fluorescence spectrophotometer with the excitation and emission wavelength bandpasses of 5 nm. The Fourier transform infrared (FT-IR) spectra were recorded on a Bruker Vertex 70 FT-IR spectrophotometer. Field-emission scanning electron microscopy (FE-SEM) images were measured on a Hitachi S-4800 microscope. Thermogravimetric analysis (TGA) was performed on a Perkin-Elmer thermal analyzer. The concentration of mercury(II) in real water samples analysis was conducted by Atomic fluorescence spectrophotometer (AFS-9700) which was made by Beijing Haiguang Co., Ltd.

2.2. Synthesis

2.2.1. Synthesis of rhodamine B hydrazide

Rhodamine B hydrazide was synthesized following the reported procedure [18].

^{1}H NMR (300 MHz, $CDCl_3$): δ = 7.95 (m, 1H), 7.47 (t, J = 3.9 Hz, 2H), 7.10–7.13 (m, 1H), 6.43–6.49 (m, 4H), 6.31 (dd, J = 2.4, J = 9.0 Hz, 2H), 3.36 (q, J = 6.9 Hz, 8H), 1.18 (t, J = 6.9 Hz, 12H).

2.2.2. Synthesis of rhodamine B Schiff base (RHO)

Rhodamine B hydrazide (0.46 g, 1 mmol) was dissolved in 7 mL of ethanol, under magnetic stirring, excess of 40% glyoxal (2 mL) mixed with ethanol (6 mL) was added, and then the solution was stirred overnight at room temperature. Large amount of saturated sodium chloride solution was added so as to obtain the pale yellow precipitate. The crude product was purified by flash column chromatography on silica gel with dichloromethane as eluent, affording 0.39 mg of compound RHO as a yellow solid (yield 77%). ^{1}H NMR (300 MHz, $CDCl_3$) δ 9.45 (d, J = 7.5 Hz, 1H), 8.03 (d, J = 0.8 Hz, 1H), 7.61–7.46 (m, 2H), 7.37 (d, J = 7.4 Hz, 1H), 7.11 (d, J = 0.5 Hz, 1H), 6.43 (dd, J = 17.0, 5.6 Hz, 4H), 6.25 (dd, J = 8.8, 2.4 Hz, 2H), 3.33 (q, J = 7.1 Hz, 8H), 1.17 (t, J = 7.1 Hz, 12H); ^{13}C NMR (75 MHz, $CDCl_3$) δ 12.57, 44.46, 66.15, 98.40, 104.07, 108.40, 124.09, 126.82, 127.55, 128.62, 134.88, 141.60, 149.26, 152.70, 152.85, 165.82, 192.60. The whole synthetic process was depicted in Scheme 1.

2.2.3. Synthesis of the silica spheres

The SiO_2 spheres were prepared according to the Stöber method [19] with mild modification. 45 mL of ethanol was firstly added to a 100 mL round-bottom flask, and then 1.8 mL H_2O, 49 mL $NH_3{\cdot}H_2O$, 4.2 mL TEOS were added respectively, the mixture was stirred gently under room temperature for 5 h. The resulting precipitant was centrifugalized for three times, and washed successively by water and ethanol.

2.2.4. Synthesis of the hybrid materials-RHO immobilized on silica spheres (Si-RH)

First, the activated silica spheres (0.65 g, 5 h at 160 °C under high vacuum) were dispersed in 70 mL of anhydrous toluene, then excess silane coupling agent of APS was added. The solution was refluxed under 110 °C for a whole day. After that, the sediment was separated out by centrifugation and washed by toluene for three times. The product was dried under vacuum for further use.

Next, RHO was grafted onto the surface of silica through APS, which could be described as follows, 0.12 g of SiO_2 and (0.2 g, 0.4 mmol) RHO were added into 50 mL round-bottom flask follow by adding 30 mL of ethanol, and then stirred by magnetic stirring bars at room temperature overnight. The precipitate was centrifuged and washed by ethanol for three times, and then dried under vacuum.

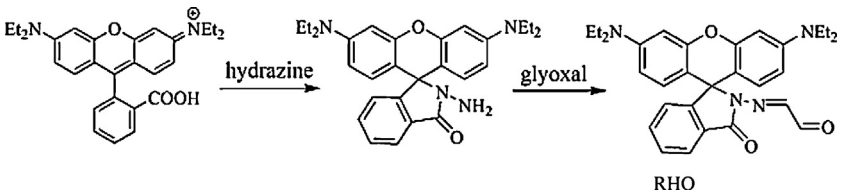

Scheme 1. Synthesis of the chemical probe RHO.

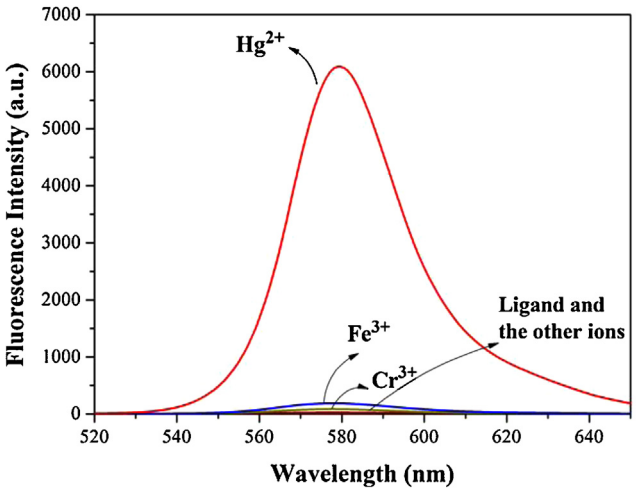

Fig. 2. Fluorescence spectra of RHO (10 μM) upon addition of 5 equiv. of various metal ions in the solution of ethanol/water (7:3, v/v).

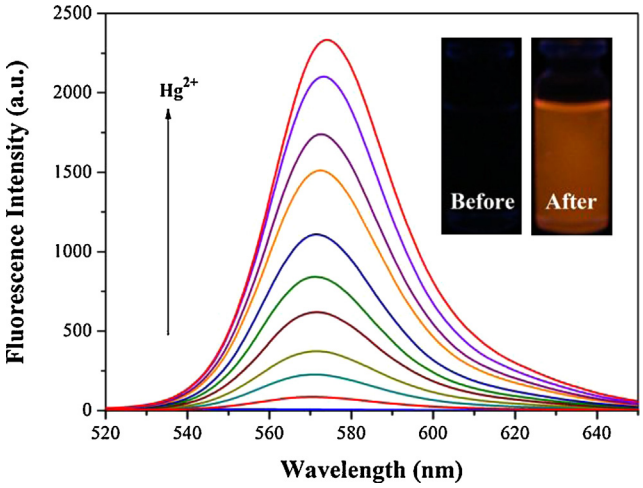

Fig. 3. The emission titration profile of RHO (10 μM) in the solution of ethanol/water (7:3, v/v) with gradually increasing the amount of Hg^{2+} (1×10^{-2} M) (λ_{ex} = 520 nm, slit: 5 nm/5 nm). Inset: the photos of RHO solution before and after the addition of Hg^{2+} ion under 365 nm UV irradiation.

2.3. Preparation of solutions for fluorescence and absorption measurements

Stock solutions (0.01 M) of K^+, Mg^{2+}, Fe^{3+}, Cd^{2+}, Zn^{2+}, Co^{2+}, Ni^{2+}, Fe^{2+}, Ca^{2+}, Hg^{2+}, Pb^{2+}, Cr^{3+}, Cu^{2+}, and Ag^+ (nitrate salts) in water were prepared. Stock solution of the host RHO (0.1 mM) was also prepared in ethanol. Test solutions were prepared by adding 300 μL of the RHO stock solution into a test tube, then placing an appropriate aliquot of each metal stock, and diluting the test solution to 3 mL with the mixture of ethanol and water. The final spectrophotometric spectra of the material were carried out in ethanol/water solution (7:3, v/v) in a quartz cell at room temperature. For all measurements, excitation wavelength was set as 520 nm, slits for both excitation and emission were 5 nm. Each spectral assay was performed in three sets and the mean value was what we utilized finally.

3. Results and discussion

3.1. Colorimetric study

The probe RHO displayed sensitive color change from colorless to pink via rhodamine lactam ring opening in presence of Hg^{2+}. The addition of 5 equiv. of other metal ions (K^+, Mg^{2+}, Fe^{3+}, Cd^{2+}, Co^{2+}, Ca^{2+}, Zn^{2+}, Ni^{2+}, Fe^{2+}, Pb^{2+}, Cr^{3+}, Cu^{2+}, and Ag^+) to the solution of RHO (10 μM) in ethanol/water (7:3, v/v) showed no color change (Fig. 1). This selective color change can be used for the "naked eye" detection of Hg^{2+} in aqueous solution.

3.2. Fluorescence study

Based on above colorimetric result, a detailed optical study was carried out to establish the selective sensing of Hg^{2+} toward RHO. The change of fluorescence spectra of RHO in the presence of various metal ions (K^+, Mg^{2+}, Fe^{3+}, Cd^{2+}, Co^{2+}, Ca^{2+}, Zn^{2+}, Ni^{2+}, Fe^{2+}, Pb^{2+}, Cr^{3+}, Hg^{2+}, Cu^{2+}, and Ag^+) in ethanol/water (7:3, v/v) solution was investigated. As shown in Fig. 2, there was almost no fluorescence when only RHO existed, which indicated that RHO was in the ring closed non-fluorescent spirolactam conformation. Significant enhancement in fluorescence intensity at 578 nm was created only upon the addition of 5 equiv. Hg^{2+} with a fluorescence quantum yield Φ = 0.64. The change of fluorescence indicated that RHO transformed from the closed spirolactam to the open ring form [20]. In the case of RHO with Hg^{2+}, remarkably enhanced fluorescence was observed at 578 nm. Only negligible emission peaks were observed after the addition of Fe^{3+} and Cr^{3+}, others ions just caused almost no fluorescence change. Therefore the probe RHO exhibited a high selectivity for Hg^{2+} over other metal ions.

The fluorescence titration of mercury(II) ion was conducted with RHO (10 μM) in ethanol/water (7:3, v/v) solution. Upon the increasing amount of Hg^{2+} (1×10^{-2} M) (0–2 equiv.), a new emission band at about 575 nm appeared with increasing intensity (Fig. 3). Moreover, an obvious color change from colorless to red under 365 nm UV irradiation was also observed in the inset in Fig. 3.

3.3. UV–vis absorption spectroscopy study

Besides the fluorescence change upon the presence of Hg^{2+} ion, the probe can also exhibit UV–vis absorbance spectra changes toward Hg^{2+} ion. As shown in Fig. 4, the UV–vis absorption spectra of RHO in solution of ethanol/water (7:3, v/v) showed no absorption spectra above 450 nm indicated the existence of closed spirolactam ring of the rhodamine fluorophore. When added 5 equiv. of various metal ions (K^+, Mg^{2+}, Fe^{3+}, Cd^{2+}, Co^{2+}, Ca^{2+}, Zn^{2+}, Ni^{2+}, Fe^{2+}, Pb^{2+}, Cr^{3+}, Hg^{2+}, Cu^{2+}, and Ag^+) to the RHO solution (10 μM)

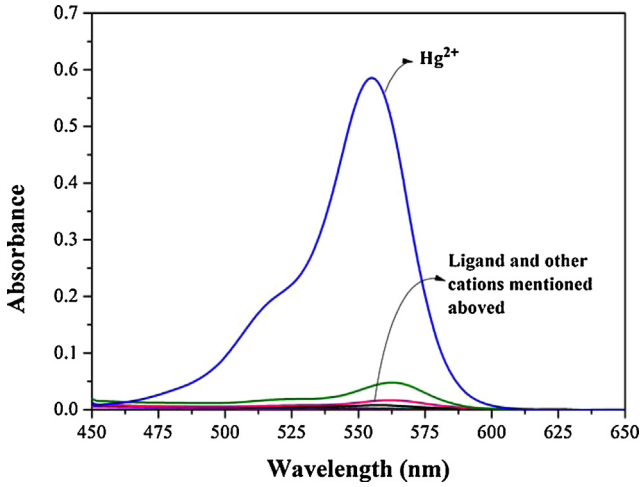

Fig. 4. UV–vis spectra of RHO (10 μM) in ethanol/water (7:3, v/v) upon addition of 5 equiv. of various metal ions (K^+, Mg^{2+}, Fe^{3+}, Cd^{2+}, Co^{2+}, Ca^{2+}, Zn^{2+}, Ni^{2+}, Fe^{2+}, Pb^{2+}, Cr^{3+}, Hg^{2+}, Cu^{2+} and Ag^+).

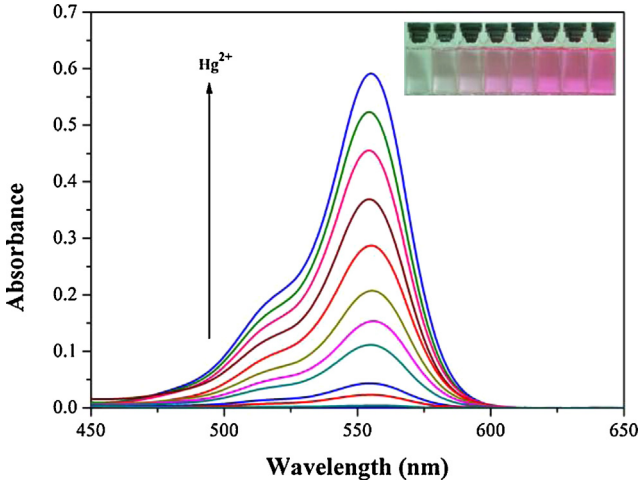

Fig. 5. The UV–vis titration profile of RHO (10 μM, 7:3, v/v) ethanol/water solution with gradual increase of Hg^{2+} (0–5 equiv.). I nset: the colorimetric performance of the solution upon adding different amount of Hg^{2+} (blank, 5, 10, 15, 20, 30, 40, 50 μM).

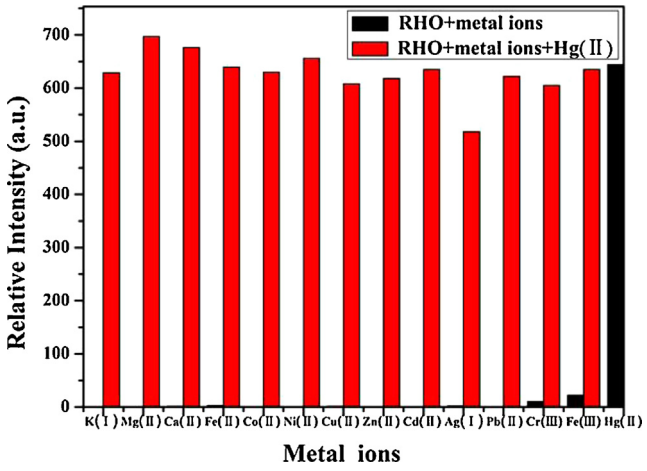

Fig. 6. The relative fluorescence intensity profiles (F/F_0) of RHO (10 μM, ethanol/water, 7:3, v/v) in the presence of 5 equiv. Hg^{2+} and the interfering ions (K^+, Mg^{2+}, Ca^{2+}, Fe^{2+}, Co^{2+}, Ni^{2+}, Cu^{2+}, Zn^{2+}, Cd^{2+}, Ag^+, Pb^{2+}, Cr^{3+}, Fe^{3+}, respectively). Black bars: the addition of Hg^{2+} and various other metal ions. Red bars: the change of the emission that occurs upon the subsequent addition of equivalent Hg^{2+} to the solution. (For interpretation of the references to color in this figure legend, the reader is referred to the web version of the article.)

in ethanol/water (7:3, v/v), only Hg^{2+} induced the sharp absorption spectrum change at 555 nm with a shoulder peak at 514 nm, which was consistent with the formation of delocalized xanthane moiety of rhodamine and the ring opening of spirolactam. Correspondingly, the solution color changed from colorless to pink in the presence of Hg^{2+} ions (Fig. 1).

Fig. 5 shows the UV–vis titration of RHO (10 μM) upon addition of 0–5 equiv. Hg^{2+}. The absorption intensity at 555 nm showed sharp increase, which was consistent with the ring opened rhodamine derivative as related reports [21,22]. The gradual color change from colorless to pink was also observed as shown by the inset of Fig. 5.

3.4. The effect of pH and response time study

We investigated the response character of RHO toward Hg^{2+} as follows. As depicted in Fig. S1 (Supporting information), after the addition of 5 equiv. Hg^{2+} to the RHO solution (10 μM, ethanol/water, 7:3, v/v), its fluorescence spectra changed from the beginning until 45 min later with the time interval of 5 min (the black squares). According to the discrete point analysis, the presence of Hg^{2+} induced gradual increment of emission peak. The fluorescence response of RHO achieved saturation in 25 min with little change as time went by. Consequently, we chose 25 min as the optimal responding time.

To apply the probe in complex environments, its response toward Hg^{2+} at different pH values was tested (Fig. S1 (Supporting information)). The pH was adjusted using diluted nitric acid or sodium hydroxide solution, no buffer was utilized to avoid the cross-contaminations. The fluorescence intensity of pure RHO did not vary with pH variation in the range of 7.0–9.0 (the red dots). However, due to the fact that proton and metal ions can both open the spirocycle and induce color changes, in the absence of Hg^{2+}, RHO also exhibited fluorescent emission with the increasing acidity (the blue triangles). The probe also showed substantially increased fluorescence in the presence of Hg^{2+}. It should be noted that, at pH higher than 7.0, the partial precipitation of HgO might decrease the actual concentration of Hg^{2+} in the sample solution, causing the decrease of fluorescence intensity of RHO–Hg^{2+} complex [23,24]. Accordingly, pH = 7.0 was chosen as the optimal test condition.

3.5. Anti-interference performance

High selectivity toward specific analyst over other competitive species is desired for any sensors. Therefore, the competition experiments were extended to various metal ions, including alkali, alkaline earth, and transition-metal ions, to evaluate the selectivity of the fluorescence chemosensor. As depicted in Fig. 6, except for the negligible spectra changes caused by Fe^{3+} and Cr^{3+}, the other competitive cations did not induce any observable fluorescence changes (the black bars). Moreover, the competition experiments revealed that the Hg^{2+}-induced fluorescence intensity was not influenced by the subsequent addition of competitive cations (the red bars). Obviously, this result confirmed that our proposed chemical probe RHO owned remarkably high selectivity toward Hg^{2+} ions over other competitive cations in aqueous solutions. The standard deviation of each spectra test was revealed in Fig. S2.A (Supporting information).

3.6. Detection limit

A good linearity between F/F_0 and concentration of Hg^{2+} in the range of $5 \times 10^{-9} - 10^{-7}$ mol/L was obtained with a linearly dependent coefficient R^2 of 0.9926 (Fig. 7). The detection limit for Hg^{2+} was calculated to be about 2.7×10^{-9} M based on $3\delta/k$ (where δ is the standard deviation of the blank solution and k is the slope of the calibration plot) [25,26].

3.7. Reversibility and possible sensing mechanism

We further carried out studies on the reversibility of the sensor to investigate if the chemical probe could be reused. The RHO–Hg^{2+} was treated with a solution of tetrabutylammonium hydroxide (TBA^+OH^-) which was used for precipitating the free mercury ions. We added 10 μM of Hg^{2+} aqueous solution to RHO solution (10 μM), and then different amount of tetrabutylammonium hydroxide TBA^+OH^- (~16 mM) were introduced. However, even excess TBA^+OH^- was added, the fluorescent emission peak induced by Hg^{2+} showed no fall. On the contrary, it appeared blue shift of 6 nm along with an increase in fluorescence intensity (Fig. S3.A (Supporting information)). In order to explain the abnormal phenomenon, we developed a contrastive test, using ethanol as

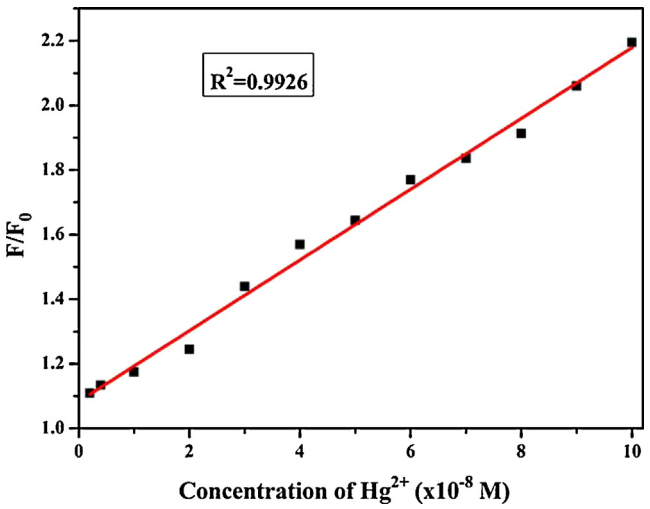

Fig. 7. The relative fluorescence intensity (F/F_0) of RHO (10 μM, 7:3, v/v) ethanol/water solution as a function of Hg^{2+} concentration in the range of $5 \times 10^{-9} - 10^{-7}$ mol/L.

the sole solvent, which means that no water was applied in the fluorescent analytical process. Under this condition, the fluorescence intensity declined dramatically as the TBA^+OH^- added (Fig. S3.B (Supporting information)). We further used excess amount of ethylenediamine tetraacetic acid disodium salt (EDTA) as chelating agent for capturing Hg^{2+}, the similar result was acquired.

From above discussion, a possible bonding mechanism was proposed as follows. Firstly, the addition of Hg^{2+} to RHO caused complexation with carbonyl O, imino N, and the terminal O atom [27]. As a result, a ring-opening of the spirolactam in rhodamine framework took place, observed by the distinct color change and fluorescence OFF–ON, as depicted in Scheme 2. Secondly, according to the irreversible analysis of the probe, a further hydrolytic process was plausible to clarify this phenomenon, which agreed with literature reports [28,29]. RHO was colorless and nonfluorescent due to the closed spirolactam ring. The addition of aqueous solution of Hg^{2+} led to spirocycle opening via coordination. But the RHO–Hg^{2+} complex was just an intermediate compound which would undergo rapid Hg^{2+}-promoted hydrolytic reaction in the presence of water. The second step (Hg^{2+} promoted hydrolysis) was based on the Hg^{2+}-promoted irreversible hydrolysis of isopropenyl acetate [30]. We anticipated that a hydrolysis reaction occurred when a similar but modified molecular moiety of isopropenyl acetate was liberated by Hg^{2+}-facilitated ring opening of the spirocycle group. Herein, Hg^{2+} acted not only as an analyte but also as the promoter for the hydrolytic reaction.

According to the analysis above, the hydrolytic process needed two factors, namely time and water. That is to say, in the solution of ethanol/water (7:3, v/v), if TBA^+OH^- was added to the RHO–Hg^{2+} complex before the hydrolytic process finished, the reversible of fluorescence could be obtained; For the second factor, water, if we performed the fluorescent titration test in absolute ethanol solution, the reversibility could be got ignoring the addition time. Therefore, we carried out further studies to prove the statement.

First, we tried to verify the effect of time. According to the analysis above, we chose 10 min as the optimal addition time in order to ensure the hydrolytic process has not finished. As shown in Fig. S4.A (Supporting information), the titration of RHO (10 μM) with Hg^{2+} (10 μM) was operated in solution of ethanol/water (7:3, v/v), then 10 min later, different amount of TBA^+OH^- (4 mM, 8 mM, 16 mM) was added, to our delight, the fluorescence spectra caused by Hg^{2+} reduced gradually as opposite to the spectra change in 40 min showed in Fig. S3.A (Supporting information).

The second factor we would prove was the effect of water. We added Hg^{2+} (10 μM) to the RHO (10 μM) in absolute ethanol solution, different time interval was allowed, that is 10 min, 25 min and 40 min, then the same amount of TBA^+OH^- (200 μL, 16 mM) was added respectively (Fig. S4.B–D (Supporting information)). Just as expected, all the emission peaks reduced apparently

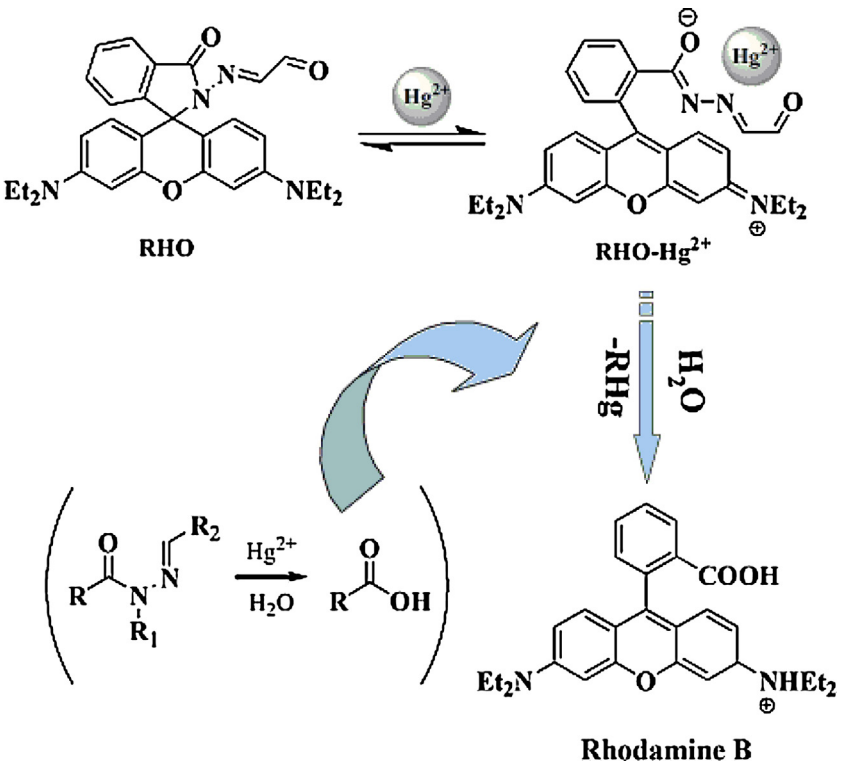

Scheme 2. Proposed binding mode and hydrolysis process of RHO with Hg^{2+}.

no matter when TBA^+OH^- was added. Consequently, from the titrimetric analysis we proved the two necessary factors which could promote the hydrolytic process. Besides, it could also be a powerful supplement for the probable mechanism we discussed, the coordination and hydrolysis process were both exist. As for the blue shift in Fig. S3.A (Supporting information), the addition of TBA^+OH^- most likely resulted in the electron transfer from the OH^- to the electron deficient imino group and the terminal carbonyl, thus enhanced the intramolecular charge transfer (ICT) process, which led to emission blue shift along with an increase in fluorescence degree just as Tang group has reported [31].

Silica spheres are suitable as host matrixes for the realization of optical chemosensors, because they are optically transparent, photophysically inert, owing a high surface-to-volume ratio as well. They also possess good water dispersibility, permeability and low toxicity [32,33]. More importantly, to avoid organic dyes leakage, their surface can be easily modified by coupling reactions with alkoxysilane derivatives [34–37]. Enlightened by above results, we further grafted the probe onto silica spheres to explore its utilization in inorganic and organic hybrid material. The synthetic route was described in Section 2. The silica spheres were prepared following the well-known Stöber method with mild modification. From Fig. S5.A (Supporting information), SEM image for the microspheres showed well monodispersed silica particles with uniformly spherical in morphology. The average diameter of the SiO_2 particles was about 2.2 μm. After the modification of SiO_2 particles with RHO, the resulting SiO_2 particles preserved its morphology well and revealed no significant size change except for the rougher surface (Fig. S5.B (Supporting information)). These monodispersed Si-RH particles represented attractive building blocks based on which luminescent materials could be constructed.

3.8. FT-IR characterization

The FT-IR spectra for RHO (a), APS modified SiO_2 particles, SiO_2-APS (b) and RHO functionalized hybrid material Si-RH (c) are showed in Fig. S6 (Supporting information). An obvious band at 1703 cm^{-1} due to the stretching vibration of —CHO of RHO appeared in Fig. S6(a) (Supporting information) The emergence of a series of bands at 2985, 2931, 2885 cm^{-1} corresponding to the vibrations of methyene —$(—CH_2—)_3$— were showed in both Fig. S6(b) and (c) (Supporting information). And the disappearance of the double absorption peaks which located between 3500 and 3300 cm^{-1} for the —NH_2 of APS in Fig. S6(c) (Supporting information) indicated the silica surface was already modified by the silane coupling agent APS. As for Fig. S6(c) (Supporting information), a new absorption peak at 1620 cm^{-1} was assigned to the grafted —N=CH— group, which demonstrated that RHO has been successfully grafted on to the surface of SiO_2. In addition, the formation of the Si—O—Si framework was evidenced by the bands of absorption of siloxane bonds which located at 1103 cm^{-1} (ν_{as}, Si—O), 803 cm^{-1}(ν_s, Si—O), and 470 cm^{-1} (δ, Si—O—Si) (ν represents stretching, δ in plane bending, s symmetric, and as asymmetric vibrations) in Fig. S6(b) and (c) (Supporting information) [38,39].

The quantity of RHO attached to the silica microspheres was estimated from the result of TGA measurement depicted in Fig. S7 (Supporting information). The TGA curve presented three main steps of thermal decomposition between 30–160 °C, 160–366 °C and 366–600 °C respectively. The endothermic process in the first step exhibited a weight loss of ca. 3.8% which could be attributed to the removal of physically absorbed water without any decomposition of chemical bonds. As for 160–366 °C, there was a large mass loss of ca. 11.2% (DTG_{max} = 336 °C) which was mainly attributed to the decomposition of the organic moiety [40,41]. The weight loss occurring between 336 °C and 600 °C was attributed to the thermal degradation of the organosilicate frameworks, involving Si—C, C—C, and C—N bond cleavage. From the second weight loss, the amount of RHO immobilizing onto the silica spheres was calculated to be about 11.2%.

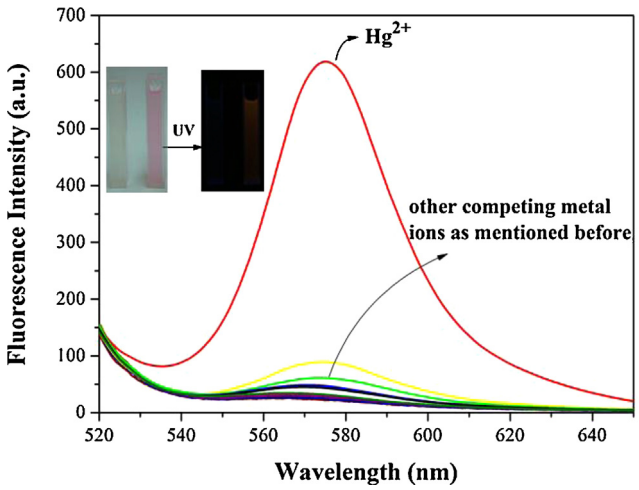

Fig. 8. Fluorescence spectra of Si-RH (0.4 mg/mL) in ethanol/water solution (7:3, v/v) in the presence of different metal ions (0.1 mM) (K^+, Mg^{2+}, Fe^{3+}, Cd^{2+}, Co^{2+}, Ca^{2+}, Zn^{2+}, Ni^{2+}, Fe^{2+}, Pb^{2+}, Cr^{3+}, Hg^{2+}, Cu^{2+}, and Ag^+, respectively). Inset: the color changes of Si-RH in aqueous solution before and after adding Hg^{2+} solution under natural light and 365 nm UV irradiation. (For interpretation of the references to color in this figure legend, the reader is referred to the web version of the article.)

The fluorescence titration curve of Si-RH (0.4 mg/mL) with different metal ions (0.1 mM) was conducted in ethanol/water (7:3, v/v). As shown in Fig. 8, upon adding various metal ions including K^+, Mg^{2+}, Fe^{3+}, Cd^{2+}, Co^{2+}, Ca^{2+}, Zn^{2+}, Ni^{2+}, Fe^{2+}, Pb^{2+}, Cr^{3+}, Hg^{2+}, Cu^{2+} and Ag^+, only Hg^{2+} could induce distinct fluorescence enhancement at 575 nm. The other competing ions just caused negligible responses. We also studied its visual colorimetric performance as shown by the inset in Fig. 8, when aqueous solution of Hg^{2+} was added, an obvious color changes from colorless to pink/red were observed by naked eyes under natural light and UV irradiation, respectively.

The effect of competing ions coexisting in the sample was also studied. As depicted in Fig. 9, except for Hg^{2+}, the other competing ions caused negligible responses to the fluorescence of Si-RH (the

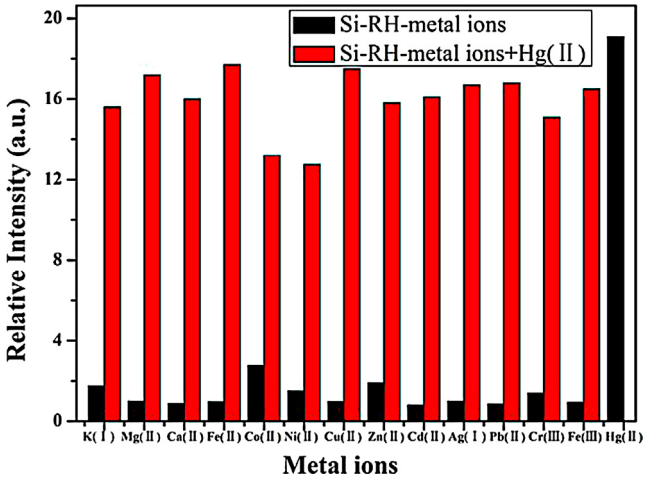

Fig. 9. The relative fluorescence intensity (F/F_0) of Si-RH (10 μM, ethanol/water, 7:3, v/v) in the presence of various cations (0.1 mM). The black bars represent the emission of Si-RH in the presence of Hg^{2+} and various other metal ions. The red bars represent the change of the emission that occurs upon the subsequent addition of equivalent Hg^{2+} to the solution. (For interpretation of the references to color in this figure legend, the reader is referred to the web version of the article.)

Table 1
Determination of Hg^{2+} in deionized water, tap water and river water samples with Atomic fluorescence spectrophotometer and RHO.

Sample	Spiked amount Hg(II) (μg/L)	Detected amount[a] Hg(II) (μg/L)	Detected amount[b] Hg(II) (μg/L)	Recovery (%)	Relative error (%)
Deionized water	17	17.09 ± 0.17	16.67 ± 0.83	98.1	−2.46
Tap water	15	14.84 ± 0.15	14.35 ± 0.78	95.7	−3.3
River water	18	17.79 ± 0.18	16.21 ± 0.97	90.1	−8.88

[a] Detected by atomic fluorescence spectrophotometer.
[b] Detected by KHO.

black bars). Moreover, only Co^{2+}, Ni^{2+} caused slight decrease of the fluorescence intensity, other spectral intensity was not influenced by the subsequent addition of Hg^{2+}. Apparently, the new probe based on inorganic–organic hybrid materials exhibited notably high selectivity toward Hg^{2+} over other competitive cations in the aqueous media. The standard deviation of each spectra test was revealed in Fig. S2.B (Supporting information).

The titration of Si-RH with different concentrations of Hg^{2+} was plotted in Fig. S8 (Supporting information), upon adding various concentration of Hg^{2+} (30–100 μM) to the Si-RH solution (0.4 mg/mL), the fluorescence intensity increased gradually, corresponding to the obvious color change from colorless to pink. It is definitely concluded that Hg^{2+} induced coordination mode as mentioned above lead to the ring-opening of the spirolactam in rhodamine framework on the surface of silica spheres, showing the distinct color change and fluorescence OFF–ON switch.

3.9. Preliminary application of RHO

In order to examine the probe RHO in practical analysis, it was applied in the determination of Hg^{2+} in deionized water, tap water and river water samples. The river water sample was obtained from Yitong River and simply filtered. All these water samples were spiked with standard Hg^{2+} solutions and then analyzed with Atomic fluorescence spectrophotometer and the proposed probe. According to Table 1, the detection results were acceptable which meant that the probe possessed potential application in real water sample detection.

4. Conclusion

In summary, a novel and simply synthesized rhodamine B Schiff base RHO targeting for highly selective and sensitive response to Hg^{2+} ion over other metal ions was developed, with the detection limit of 2.7×10^{-9} M. It exhibited distinct Hg^{2+}-induced increase in the intensity of both fluorescent emission and absorbance bands together with apparent color change from colorless to pink which also provided "naked eye" detection. The functional mode was based on a proposed Hg^{2+}-promoted hydrolysis mechanism in ethanol–water mixtures. Moreover, we further grafted RHO onto silica spheres, the obtained inorganic–organic hybrid material exhibited excellent selectivity for Hg^{2+} as well, which could endow the system with potential applications in molecular level sensor devices, our study provided a commendable candidate for constructing chemosensor for mercury(II).

Acknowledgments

The authors gratefully thank the financial supports of the NSFC (Grant nos. 51172224 and 51103145) and the Science and Technology Developing Project of Jilin Province (Grant nos. 20100533 and 201201009).

Appendix A. Supplementary data

Figures giving fluorescence spectra, UV–vis spectra, SEM image, FT-IR spectra and TGA analysis.

Supplementary data associated with this article can be found, in the online version, at http://dx.doi.org/10.1016/j.snb.2013.06.011.

References

[1] J.M. Benoit, W.F. Fitzgerald, A.W. Damman, The biogeochemistry of an ombrotrophic bog: evaluation of use as an archive of atmospheric mercury deposition, Environmental Research: Section A 78 (1998) 118–133.
[2] A. Benzoni, F. Zino, E. Franchi, Mercury levels along the food chain and risk for exposed populations, Environmental Research: Section A 77 (1998) 68–72.
[3] E.M. Nolan, S.J. Lippard, Tools and tactics for the optical detection of mercuric ion, Chemical Reviews 108 (2008) 3443–3480.
[4] B.R. Von, Toxicology update, Journal of Applied Toxicology 15 (1995) 483–493.
[5] H.H. Harris, I.J. Pickering, G.N. George, The chemical form of mercury in fish, Science 301 (2003) 1203.
[6] Y. Hong, S. Chen, C.W.T. Leung, J.W.Y. Lam, J. Liu, N.W. Tseng, R.T.K. Kwok, Y. Yu, Z. Wang, B.Z. Tang, Fluorogenic Zn(II) and chromogenic Fe(II) sensors based on terpyridine-substituted tetraphenylethenes with aggregation-induced emission characteristics, ACS Applied Materials & Interfaces 3 (2011) 3411–3418.
[7] Y. Gong, X. Zhang, C. Zhang, A. Luo, T. Fu, W. Tan, G. Shen, R. Yu, Through bond energy transfer: a convenient and universal strategy toward efficient ratiometric fluorescent probe for bioimaging applications, Analytical Chemistry 84 (2012) 10777–10784.
[8] X. Lu, Z. Guo, M. Feng, W. Zhu, Sensing performance enhancement via acetate-mediated N-acylation of thiourea derivatives: a novel fluorescent turn-on Hg^{2+} chemodosimeter, ACS Applied Materials & Interfaces 4 (2012) 3657–3662.
[9] Q. Zou, H. Tian, Chemodosimeters for mercury(II) and methylmercury(I) based on 2,1,3-benzothiadi-azole, Sensors and Actuators B 149 (2010) 20–27.
[10] Y. Jeong, J. Yoon, Recent progress on fluorescent chemosensors for metal ions, Inorganica Chimica Acta 381 (2012) 2–14.
[11] X. Cheng, R. Tang, H. Jia, J. Feng, J. Qin, Z. Li, New fluorescent and colorimetric probe for cyanide: direct reactivity, high selectivity, and bioimaging application, ACS Applied Materials & Interfaces 4 (2012) 4387–4392.
[12] J.R. Lakowicz, Principles of Fluorescence Spectroscopy, third ed., Springer, New York, 2006, pp. 67–69.
[13] H.N. Kim, M.H. Lee, H.J. Kim, J.S. Kim, J. Yoon, A new trend in rhodamine-based chemosensors: application of spirolactam ring-opening to sensing ions, Chemical Society Reviews 37 (2008) 1465–1472.
[14] X. Chen, T. Pradhan, F. Wang, J.S. Kim, J. Yoon, Fluorescent chemosensors based on spiroring-opening of xanthenes and related derivatives, Chemical Reviews 112 (2012) 1910–1956.
[15] M.H. Lee, J.S. Wu, J.W. Lee, J.W. Jung, J.S. Kim, Highly sensitive and selective chemosensor for Hg^{2+} based on the rhodamine fluorophore, Organic Letters 9 (2007) 2501–2504.
[16] Z.Q. Hu, C.S. Lin, X.M. Wang, L. Ding, C.L. Cui, S.F. Liu, H.Y. Lu, Highly sensitive and selective turn-on fluorescent chemosensor for Pb^{2+} and Hg^{2+} based on a rhodamine–phenylurea conjugate, Chemical Communications 46 (2010) 3765–3767.
[17] J.H. Soh, K.M.K. Swamy, S.K. Kim, S. Kim, S.H. Lee, J. Yoon, Rhodamine urea derivatives as fluorescent chemosensors for Hg^{2+}, Tetrahedron Letters 48 (2007) 5966–5969.
[18] V. Dujols, F. Ford, A.W. Czarnik, A long-wavelength fluorescent chemodosimeter selective for Cu(II) ion in water, Journal of the American Chemical Society 119 (1997) 7386–7387.
[19] W. Stöber, A. Fink, E. Bohn, Controlled growth of monodisperse silica spheres in the micron size range, Journal of Colloid and Interface Science 26 (1968) 62–69.
[20] J. Zhang, B. Li, L. Zhang, H. Jiang, An optical sensor for Cu(II) detection with upconverting luminescent nanoparticles as excitation source, Chemical Communications 48 (2012) 4860–4862.
[21] V. Bhalla, R. Tejpal, M. Kumar, Rhodamine appended terphenyl: a reversible off–on fluorescent chemosensor for mercury ions, Sensors and Actuators B 151 (2010) 180–185.

[22] X. Lou, L. Qiang, J. Qin, Z. Li, A new rhodamine-based colorimetric cyanide chemosensor: convenient detecting procedure and high sensitivity and selectivity, ACS Applied Materials & Interfaces 1 (2009) 2529–2535.
[23] L. Feng, H. Li, Y. Lv, Y. Guan, Colorimetric and turn-on fluorescent determination of Cu^{2+} ionbased on rhodamine–quinoline derivative, Analyst 137 (2012) 5829–5833.
[24] Z.X. Han, X.B. Zhang, Z. Li, G.J. Mao, Z. Jin, G.L. Shen, R.Q. Yu, X.Y. Wu, A highly sensitive quinoline-containing rhodamine B thiohydrazide based fluorescent probe for Hg^{2+} in aqueous solution and living cells, Analytical Letters 43 (2010) 2751–2761.
[25] J. Zhang, C. Yu, S. Qian, G. Lu, J. Chen, A selective fluorescent chemosensor with 1, 2, 4-triazole as subunit for Cu(II) and its applications in imaging Cu(II) in living cells, Dyes and Pigments 92 (2012) 1370–1375.
[26] C. Kar, M.D. Adhikari, A. Ramesh, C. Das, NIR- and FRET-Based sensing of Cu^{2+} and S^{2-} in physiological conditions and in live cells, Inorganic Chemistry 52 (2013) 743–752.
[27] Q.J. Ma, B.X. Zhang, X.H. Zhao, Z. Jin, G.J. Mao, G.L. Shen, R.Q. Yu, A highly selective fluorescent probe for Hg^{2+} based on a rhodamine–coumarin conjugate, Analytica Chimica Acta 663 (2010) 85–90.
[28] J. Du, J. Fan, X. Peng, P. Sun, J. Wang, H. Li, S. Sun, A new fluorescent chemodosimeter for Hg^{2+}: selectivity, sensitivity, and resistance to Cys and GSH, Organic Letters 12 (2010) 476–479.
[29] L. Wang, J. Yan, W. Qin, W. Liu, R. Wang, A new rhodamine-based single molecule multianalyte (Cu^{2+}, Hg^{2+}) sensor and its application in the biological system, Dyes and Pigments 92 (2012) 1083–1090.
[30] P. Abley, J.E. Byrd, J. Halpern, Mercury(II)- and thallium(II)-catalyzed hydrolysis of isopropenyl acetate, Journal of the American Chemical Society 94 (1972) 1985–1989.
[31] W. Wu, Z. Sun, Y. Zhang, J. Xu, H. Yu, X. Liu, Q. Wang, W. Liu, Y. Tang, A multifunctional nanosensor based on silica nanoparticles and biological applications in living cells, Chemical Communications 48 (2012) 11017–11019.
[32] X. Fang, C. Chen, Z. Liu, P. Liu, N. Zheng, A cationic surfactant assisted selective etching strategy to hollow mesoporous silica spheres, Nanoscale 3 (2011) 1632–1639.
[33] S. Bonacchi, D. Genovese, R. Juris, M. Montalti, L. Prodi, E. Rampazzo, N. Zaccheroni, Luminescent silica nanoparticles: extending the frontiers of brightness, Angewandte Chemie International Edition 50 (2011) 4056–4066.
[34] E. Mahon, D.R. Hristov, K.A. Dawson, Stabilising fluorescent silica nanoparticles against dissolution effect for biological studies, Chemical Communications 48 (2012) 7970–7972.
[35] B. Lei, B. Li, H. Zhang, S. Lu, Z. Zheng, W. Li, Y. Wang, Mesostructured silica chemically doped with Ru^{II} as a superior optical oxygen sensor, Advanced Functional Materials 16 (2006) 1883–1891.
[36] L. Wang, B. Li, L. Zhang, L. Zhang, H. Zhao, Fabrication and characterization of a fluorescent sensor based on Rh 6G-functionlized silica nanoparticles for nitrite ion detection, Sensors and Actuators B 171 (172) (2012) 946–953.
[37] K. Sarkar, K. Dhara, M. Nandi, P. Roy, A. Bhaumik, P. Banerjee, Selective zinc(II)-ion fluorescence sensing by a functionalized mesoporous material covalently grafted with a fluorescent chromophore and consequent biological applications, Advanced Functional Materials 19 (2009) 223–234.
[38] Y. Li, B. Yan, J.L. Liu, Luminescent organic–inorganic hybrids of functionalized mesoporous silica SBA-15 by thio-salicylidene Schiff base, Nanoscale Research Letters 5 (2010) 797–804.
[39] B. Levasseur, A.M. Ebrahim, T.J. Bandosz, Interactions of NO_2 with amine-functionalized SBA-15: effects of synthesis route, Langmuir 28 (2012) 5703–5714.
[40] E.J. Kim, S.M. Seo, M.L. Seo, H.J. Jung, Functionalized monolayers on mesoporous silica and on titania nanoparticles for mercuric sensing, Analyst 135 (2010) 149–156.
[41] Y.J. Li, B. Yan, Lanthanide (Eu^{3+}, Tb^{3+})/β-diketone modified mesoporous SBA-15/organic polymer hybrids: chemically bonded construction, physical characterization, and photophysical properties, Inorganic Chemistry 48 (2009) 8276–8285.

Biographies

Jingkai Ni received his BSc in 2010 from Inner Mongolia University for the Nationalities, and then he began his MSc and PhD student experience in condensed state physics in Changchun Institute of Optics Fine Mechanics and Physics of Chinese Academy of Sciences (CIOMP) under the supervising of Prof. Bin Li. His research interests mainly on the synthesis of optical and chemical sensing materials.

Qiuyan Li works as an associate professor at Changchun institute of engineering technology, her current research interest is the technology of database.

Bin Li received his BSc in 1986 and MSc in 1991 in Northeast Normal University (NNU), and PhD in Changchun Institute of Applied Chemistry of Chinese Academy of Sciences (CAS). He became a postdoc in Jilin University and then joined the research group of Prof. V.W.W. Yam as a research assistant at Department of Chemistry of Hong Kong University. Presently, he works as an associate professor at NNU and researcher at CIOMP of CAS. His current research interests focus on the applications of optical sensing materials and organic light emitting devices.

Liming Zhang received his BSc in 2005 from Northeast Normal University (NENU) and PhD in 2010 in condensed state physics in Changchun Institute of Optics Fine Mechanics and Physics of Chinese Academy of Sciences (CIOMP), and then he became an associate research fellow at CIOMP. His research interest is luminescent materials and molecular probe.